

Monitoring land cover change and its dynamic mechanism on the Qehan Lake Basin, Inner Mongolia, North China, during 1977–2013

Xi Chun  · Mei Yong · Jiyao Liu · Wenjun Liang

Received: 7 August 2017 / Accepted: 27 February 2018 / Published online: 9 March 2018
© Springer International Publishing AG, part of Springer Nature 2018

Abstract The Qehan Lake Basin is located in the north of the Otindag Sandy Land, where the fragile eco-environment is sensitive to climate change and human activity. We analyzed land cover change and the concomitant processes of ecological change based on multi-spectral scanning (MSS), thematic mapper (TM), and enhanced TM (ETM+) images. The results showed that from 1977 to 2000, the area of dune sand increased significantly by 840.2 km², while the area of high cover grassland (HCGL), medium cover grassland (MCGL), and low cover grassland (LCGL) reduced by 140.6, 207.3, and 463.3 km², respectively. Additionally, the area of wetland decreased by 112.9 km². During the period of 1977 to 2000, the land cover condition index (LCCI) reached a low of 27.7, which indicated serious eco-environmental challenges in the Qehan Lake watershed. However, the process of desertification was reversed, and vegetation cover was gradually restored

after 2000. From 2000 to 2013, the area of LCGL increased by 369.2 km² (13.4%), while the area of dune sand decreased by 560.1 km² (29.4%). The LCCI improved to reach 29.18 in 2013, demonstrating a significant eco-environmental improvement. Although climate change, human activity, and ecological policies have together determined the scope and extent of desertification in the watershed, the most fundamental factor in the restoration of vegetation was precipitation.

Keywords Land use and land cover · Arid environment · Eco-environment · Otindag Sandy Land · GIS

Introduction

Land use and land cover (LULC) change is recognized as a key component in global change and has attracted increasing attention in recent decades (Verburg et al. 2011; Matthews et al. 2004). LULC undergoes rapid variations at different spatial and temporal scales, and not only affects regional sustainable development, but also impacts on global change to the same extent as natural elements (Veldkamp and Lambin 2001). It has become the main contributor to ecosystem change in arid China (Yin et al. 2018; Zheng et al. 2006; Zhao et al. 2013; Mu et al. 2013).

The Otindag Sandy Land (OSL), which is located in an arid to semi-arid climate transition zone, with a very fragile ecosystem, is sensitive to global changes (Liu et al. 2008; Xiao et al. 1995; Yu et al. 2004; Yang et al. 2007). It is believed by many investigators that the

X. Chun (✉) · J. Liu · W. Liang
Inner Mongolia Key Laboratory of Mongolian Plateau
Environment and Global Change, Inner Mongolia Normal
University, 81 Zhaowuda Road, Hohhot, Inner Mongolia 010022,
China
e-mail: chunxinmg@163.com

X. Chun · J. Liu · W. Liang
Inner Mongolia Repair Engineering Laboratory of Wetland
Eco-environment System, Inner Mongolia Normal University, 81
Zhaowuda Road, Hohhot, Inner Mongolia 010022, China

M. Yong
College of Geography Science, Inner Mongolia Normal
University, 81 Zhaowuda Road, Hohhot, Inner Mongolia 010022,
China

degradation of the eco-environment in the OSL is due to continued high temperatures, droughts (Yang et al. 2007; Ye et al. 2000), and strong winds (Wang et al. 2006, 2007a, 2009), resulting in the area of dune sand increasing rapidly, followed by a severe wetland shrinkage and a serious degradation of vegetation. It has become one of the most seriously desertified regions in China, with extensive eco-environmental deterioration, and is an important source area for dust storms. However, other investigators believe that inappropriate human economic activity has caused the destruction of grassland and the consequent deterioration in the eco-environment (Liu and Wang 2007; Li et al. 2011; Lin et al. 2012; Peng et al. 2007; Mason et al. 2008; Niu et al. 2005; Zhao et al. 2005; Zheng et al. 2006). Although the process of land desertification has been reversed over the last 10 years (Mu et al. 2013; Wu et al. 2013), the region still faces a grim ecological future. Studies of the deterioration of the eco-environment in the OSL have been conducted from different perspectives, but there has been a lack of studies at the watershed scale. The river-lake system in the watershed provides the necessary water for vegetation growth and desert reversal; however, the system is very sensitive to climate change and human activity. LULC change involves intuitive changes in the terrestrial ecosystem pattern, structure, land use types, and characteristics regarding their interaction between climate and human disturbance (Li et al. 2009; Yan et al. 2009; Zhao et al. 2013). However, studies using a combination of land cover condition index (LCCI) analysis

and a time series of Landsat image data over a long time span are relatively scarce.

The aims of this study were to (i) use remote sensing and geographic information system (GIS) images to monitor land cover changes during 1977–2013 and (ii) explore natural and anthropogenic drivers of land cover in the study area.

Materials and methods

Study area

Qehan Lake Basin (QLB), located in the north of the OSL in Inner Mongolia, has an area of 14,212 km². The area is an arid to semi-arid climate transition zone (Fig. 1a). The basin is distributed at an altitude from 1400 m above sea level in the south to 1000 m in the north and the ground undulates gently. The terrain from north to south is marked by the formation of tableland, lowland, and sandy landscapes (Fig. 1b). The mean annual temperature (MAT) in the QLB was 2.3 °C during 1955–2013. In summer, the area is affected by the monsoon system and is hot and rainy, with a maximum temperature of 39.1 °C. In winter, the area is influenced by the Mongolian high-pressure system, and the climate is dry and cold. The extreme minimum temperature recorded in the QLB was −42.2 °C, while the average annual wind speed is 5.0 m/s, with a maximum of 32.3 m/s. The mean annual precipitation (MAP) is approximately 280 mm, of which about 70% occurs from

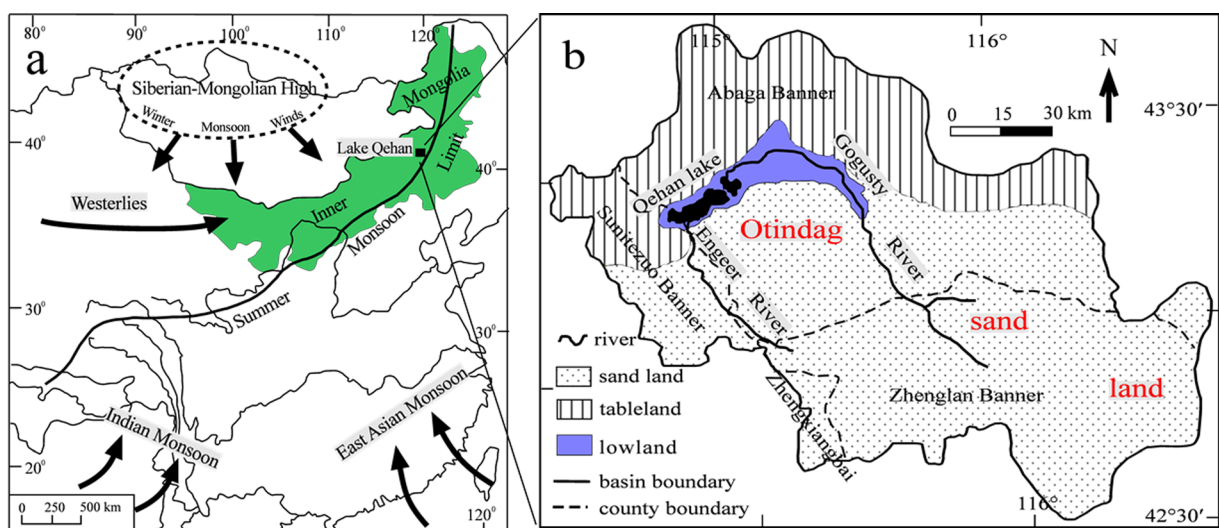


Fig. 1 a Map of the study area and b QLB

June to August. The MAP decreases from 350 to 400 mm in the southeast to 150–200 mm in the north-west (Chun et al. 2017). The QLB is located in the Xilingol League and includes part of the Banners of Abaga, Zhenglan, Zhengxiangbai, and Sunitezuo. Qehan Lake is located in the center of the QLB and is fed by the Gogusty and Engeer rivers, which flow into it from the south, forming a series of chain-like lakes. In addition, as an important water source, it is not only essential to the daily life of local residents, but is also a natural barrier protecting the ecosystem of the Xilingol grasslands. The total population of the QLB is approximately 38,000, with most inhabitants surviving by grazing livestock. The main plants in the grassland and sandy land areas are *Leymus chinense*, *Stipa krylovii*, *Caragana microphylla* Lam, *Setaria* spp., *Artemisia* spp., *Ulmus pumila* var. *Sabulosa*, *Salix flavida*, *Salix microstachya*, *Elaeagnus angustifolia*, and *Lespedeza bicolor* Turcz (Chinese Academy of Sciences Fieldwork group in Inner Mongolia and Ningxia 1985).

Data sources and processing

The study was conducted using multi-temporal and multi-resolution images from Landsat multi-spectral scanning (MSS), thematic mapper (TM), and enhanced TM (ETM+), which were collected (<http://gloris.usgs.gov>) in July and August (Table 1). All downloaded remote sensing images had the Universal Transverse Mercator Projection of zone 49 N, with WGS 84 geographic coordinates. Topographic maps with a 1:50,000 scale were used to register the selected remote sensing images to a Gauss-Kruger projection, with Beijing 54 geographic coordinates. The images were a standard pseudo color composite of bands 7, 5, and 4 for MSS, and bands 4, 3, and 2 for TM/ETM+. For each image scene, a sub-image covering the study area was clipped from the larger original image and edges were enhanced by gray-scale transformation (Lu et al. 2004; Liu et al.

2008). The images were geometrically rectified to the local coordinate system of QLB using 40 ground control points symmetrically distributed across the images. Visual interpretation was based on image characteristics, such as color, shape, size, shading, texture, structure, and the relative spatial distribution of each class of land cover. In addition, the ancillary materials mentioned above were used to improve the accuracy of the classification. Using 30-m resolution images from Landsat in 2013 as a basic data resource, we acquired land cover classification data from 1977, 1987, 2000, 2007, 2010, and 2013 by visual interpretation. A third-order polynomial and nearest neighbor approach was applied to achieve the geometric accuracy within half a pixel. Spatio-temporal transfer data were obtained by overlying 1977, 1987, 2000, 2007, 2010, and 2013 images with the basic data, respectively.

The flowchart of the image processing techniques is shown in Fig. 2. The other data used in this study for reference and analysis included (1) monthly temperature, precipitation, and wind data from four stations near the watershed, which was obtained from the Inner Mongolia weather survey (Table 2) and (2) population and livestock data derived from all administrative districts (Sumos) in the catchment, with sheep used as the unit of livestock (for example, one cattle, one horse, and one camel were equal to 5, 6, and 7 sheep, respectively).

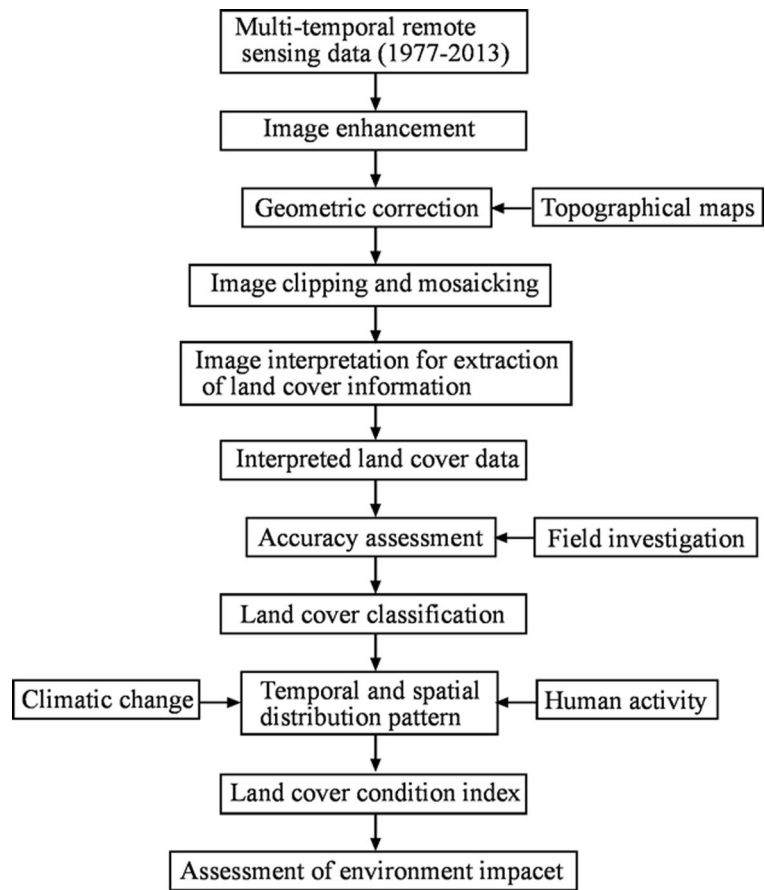
Methods

Land cover classification

To describe the various types of land cover in the QLB more accurately, this study combined the features of the multiform landscapes of the OSL with the elm-scrub woodlands and mixed-growth shrub land in the grasslands of the region. This formed a large area of shrub-woodland. The woodland categories mainly included

Table 1 Remote sensing data, population, and livestock record used in the QLB

| Materials | Date(s) | Region | Characteristic | Resolution |
|-----------------------|------------------------------------|-----------|-------------------------------|-------------|
| LandSat_MSS | 25/07/1977, 06/07/1987 | Watershed | Cloud-free days | 80 × 80 m |
| LandSat5_TM | 05/07/2010 | Watershed | Cloud-free days | 30 × 30 m |
| LandSat7_ETM+ | 01/07/2000, 06/08/2007, 05/07/2013 | Watershed | Cloud-free days | 30 × 30 m |
| Topographic maps | 1959 | Watershed | 1:50000 | |
| Human activities data | 1955–2013 | Watershed | Population, livestock numbers | Sumo’s data |

Fig. 2 The flowchart showing methodology of the study

elm from the *C. microphylla* Lam, *S. flavida*, *S. microstachya*, and *L. bicolor* Turcz families (Chinese Academy of Sciences Fieldwork group in Inner Mongolia and Ningxia 1985). According to the characteristics of the catchment eco-environment, we classified twelve types of land cover: woodland, elm-scrub woodland, high cover grassland (HCGL), medium cover grassland (MCGL), low cover grassland (LCGL), water area, swamp land, dune sand, saline land, arable land, residential land, and transportation land. Construction land was included within the residential and

transportation land categories. Wetland was included within the water area and swamp land categories.

In this study, the visual interpretation classification method was used to classify the individual images independently. To identify the land cover classification, we conducted a field investigation using 40 vegetation plots of 30 m × 30 m from July 2010 to August 2013, respectively. These plots were distributed across the QLB and included all the land cover types. At each location, species percentage cover, the dominant species, vegetation height, photographs of the vegetation, the degree of

Table 2 Meteorological sites information around the QLB

| Station | Location | Elevation (m) | Mean temperature (°C) | Mean precipitation (mm) | Period |
|----------------------|-----------------------|---------------|-----------------------|-------------------------|-----------|
| Abaga Banner | 44° 01' N, 114° 57' E | 1126.1 | 1.30 | 241.2 | 1953–2013 |
| Zhenglan Banner | 42° 18' N, 116° E | 1301 | 2.30 | 357.6 | 1971–2013 |
| Zhengxiangbai Banner | 42° 18' N, 115°E | 1347.8 | 2.39 | 354.8 | 1971–2013 |
| Sunidzuo Banner | 43° 52' N, 113° 38'E | 1036.7 | 3.09 | 191.1 | 1956–2013 |

desertification, and vegetation phenology were recorded. When an land cover type transition area with differences in the dominant vegetation community was found, the researchers walked along the boundary of the area with a GPS recorder to delineate the corresponding boundary and transferred the sample plots to the overlying images by ArcGIS software. These data were used to analyze the characteristics of a Landsat image series for different land cover types and then to develop a classification method. To identify the magnitude of the land cover conversions, we performed sensitivity analyses using calibration samples to determine the magnitude of the optimal change for each land cover conversion.

We implemented a stratified random sampling design to determine the proportion of each land type and collected 2000 random samples (in theory the minimum number of samples was 1998 for a 95% confidence level and the maximum permissible relative error was 0.01 for a 30 m × 30 m plot) in the study area (Olofsson et al. 2014). To classify the images from Landsat ETM+ 2013, 500 training samples were used in combination with field data. All the training sites were tested for signature separability based on the transformed divergence value. The reference data were derived from a visual interpretation of random samples taken at the same time by high-resolution Google Earth imagery (Olofsson et al. 2014). We generated 1500 verified samples at the Landsat ETM+ pixel size based on land cover in 2013. Our classified land cover and Google Earth maps for each class in 2013 had an average user’s and producer’s accuracy of 81.4 and 77.6% (Table 3), respectively. In conclusion, elm-scrub woodland, water area, swamp land, dune sand, saline land, residential land, and transportation land were consistently mapped with a relatively high accuracy. In contrast, woodland and grassland were generally mapped with a lower reliability. It may be that the spectral and phonological similarity of HCGL, MCGL, and LCGL resulted in higher mapping errors for these classes.

We could not verify the Landsat MSS image classification accuracy because of the lack of Google Earth image data in 1977, but local historical documents, which were basically consistent with the Landsat MSS image data, also indicated the condition of the environment at the same time (Chinese Academy of Sciences Fieldwork group in Inner Mongolia and Ningxia 1985; Department of Animal Husbandry Compilation History Commission 1997).

Land cover transition matrix

After transforming the link between the two periods of different land cover, the results gained could be used in the quantitative analysis of a land cover transition matrix, with access to land transition cases for each period, thus:

$$A_{ij} = \begin{bmatrix} A_{11} & A_{12} & \dots & A_{1n} \\ A_{21} & A_{22} & \dots & A_{2n} \\ \dots & \dots & \dots & \dots \\ A_{n1} & A_{n2} & \dots & A_{nn} \end{bmatrix}$$

where n is a land cover type number. A_{ij} refers to the area with i land types in period K shifting into j land types in period $K + 1$.

LCCI

Land cover change is a direct representation of regional ecosystem patterns and structure types, which reflect the ecosystem community composition, quality of the ecosystem, ecological service function and evaluation, and environmental condition. Wetland, woodland, and grassland ecosystems have a unique value in China in terms of their ecological services (Chen and Zhang 2000; Xie et al. 2010). Land cover categories have a corresponding relationship with ecosystem types (Bai et al. 2014; Xu et al. 2003). According to the land cover condition of the study area, we selected five specific land cover types (woodland, elm-scrub woodland, HCGL, water area, and swamp land) to determine an LCCI to reflect the land cover ecosystem condition, which would indicate the service function of the ecosystem. The higher the index, the stronger the ecosystem and the better supported its regulation and functionality. The index was expressed as:

$$Z = \left(\frac{\sum_i^5 C_i}{A} \right) \times 100\%$$

where Z represents the LCCI; C_i represents the area of woodland, elm-scrub woodland, HCGL, water area, and swamp land ($i = 1, 2, \dots, 5$ land cover types); and A represents the total area of the region.

Principal component analysis (PCA)

PCA is a statistical method for reducing data and identifying the components that account for the overall

Table 3 Error matrix Google earth and Landsat land cover in QLB for based on the validation (75%)

| Reference land cover (from Google earth interpretation) | | | | | | | | | | | | | | |
|---|-----------|---------------------|------|------|------|------------|------------|-----------|-------------|-------------|------------------|---------------------|-------|---------------------|
| | Wood land | Elm- scrub woodland | HCGL | MCGL | LCGL | Water area | Swamp land | Dune sand | Saline land | Arable land | Residential land | Transportation land | Total | User's accuracy (%) |
| land cover | 10 | 4 | 0 | 0 | 0 | 0 | 0 | 0 | 0 | 0 | 0 | 0 | 14 | 71.4 |
| Woodland | | | | | | | | | | | | | | |
| Elm- scrub woodland | 9 | 136 | 21 | 1 | 0 | 0 | 0 | 0 | 0 | 0 | 0 | 0 | 167 | 81.4 |
| HCGL | 0 | 26 | 184 | 20 | 4 | 0 | 2 | 0 | 0 | 0 | 0 | 0 | 236 | 78.0 |
| MCGL | 0 | 0 | 105 | 356 | 89 | 0 | 0 | 0 | 0 | 0 | 0 | 0 | 550 | 64.7 |
| LCGL | 0 | 0 | 35 | 86 | 205 | 0 | 0 | 4 | 0 | 0 | 0 | 0 | 330 | 62.1 |
| Water area | 0 | 0 | 0 | 0 | 0 | 16 | 0 | 0 | 0 | 0 | 0 | 0 | 16 | 100 |
| Swamp | 0 | 0 | 1 | 0 | 0 | 0 | 4 | 0 | 0 | 0 | 0 | 0 | 5 | 80.0 |
| Dune sand | 0 | 0 | 0 | 0 | 0 | 0 | 0 | 139 | 3 | 0 | 0 | 0 | 142 | 97.9 |
| Saline land | 0 | 0 | 0 | 0 | 0 | 1 | 0 | 2 | 30 | 0 | 0 | 0 | 33 | 90.9 |
| Arable land | 0 | 0 | 0 | 0 | 0 | 0 | 0 | 0 | 0 | 1 | 0 | 0 | 1 | 100 |
| Residential land | 0 | 0 | 0 | 0 | 0 | 0 | 0 | 0 | 0 | 1 | 1 | 0 | 2 | 50.0 |
| Transportation land | 0 | 0 | 0 | 0 | 0 | 0 | 0 | 0 | 0 | 0 | 0 | 5 | 5 | 100 |
| Total | 19 | 166 | 346 | 463 | 298 | 17 | 6 | 145 | 33 | 2 | 1 | 5 | 1500 | 81.4 |
| Producer's accuracy (%) | 52.6 | 81.9 | 53.2 | 76.9 | 68.8 | 94.1 | 66.7 | 95.9 | 90.9 | 50.0 | 100 | 100 | 77.6 | |

variability within the variables taken into consideration (De Coster et al. 1998). The original parameters can be rearranged into several new uncorrelated comprehensive components (or factors) without losing significant information (Brown 1998). Every new component is the linear combination of the original variables and is unrelated, which makes it possible to accurately describe the characteristics of the analyzed data. The calculated factors are rotated by a varimax rotation, thus strengthening the loadings of closely related variables in each factor. Each component describes a certain amount of the statistical variance of the analyzed data and is interpreted according to the inter-correlated variables. Variable loadings are defined by the orthogonal projection of the variables on each of the factors. The selection of the factors is based on both the significance of the factor and the cumulative percentage of the data variance it explains (Petrisor et al. 2012; Hatcher 1994). Hence, in this study we selected human activity (livestock and population) and climate change (mean annual precipitation, temperature, wind speed, and wind days) as factors to analyze the dynamic mechanism of LULC change.

Results

Land cover change

The area of watershed grassland decreased from 10,903.4 km² in 1977 to 10,564.4 km² in 2013, i.e., a

degraded area of 339 km² (3.1%) (Table 4). The area of HCGL, MCGL, and LCGL decreased by 51.6, 193.3, and 94.1 km², respectively. Similarly, the area of water land and swamp land decreased by 27.3 and 41.9 km² (15.3 and 45.4%), respectively. The area of dune sand and saline land increased by 280.1 and 45.7 km² (26.3 and 16.9%), respectively. The eco-environment damaged in recent decades was still in its primary recovery stage and was extremely fragile and unstable. The area of woodland and elm-shrub woodland increased by 7.7 and 33.3 km², respectively. Some of eco-adjustment functionalities were limited. Table 5 shows that the LCCI was 29.18 in 2013, which was still below the 29.74 recorded in 1977, confirming the current reality of the fragile eco-environment in the watershed. The area of arable land, residential land, and transport land was 24.1, 7.1, and 45.8 km² in 2013 (Table 4), respectively. These land use types increased by 412.8, 77.5, and 70.3%, respectively, which highlighted the intensity of human activity in the area. However, these areas still only accounted for 0.54% of the total watershed area in 2013, which was insufficient to influence the formation and evolution of the watershed landscape pattern.

Spatio-temporal land cover patterns

The dynamic process of land cover change reflects the environmental degradation of an extremely fragile ecology in the QLB. Eco-environmental degradation

Table 4 Land cover change in QLB from 1977 to 2013 (unit: km²)

| Land cover type | Time | | | | | |
|----------------------------------|--------|--------|--------|--------|--------|--------|
| | 1977 | 1987 | 2000 | 2007 | 2010 | 2013 |
| Woodland | 124.9 | 106.6 | 105.4 | 111.9 | 130.3 | 132.6 |
| Elm-scrub woodland | 1543.4 | 1530.1 | 1526.1 | 1530.6 | 1580.8 | 1576.7 |
| High coverage grassland (HCGL) | 2288.0 | 2241.3 | 2147.4 | 2239.9 | 2233.0 | 2236.4 |
| Medium coverage grassland (MCGL) | 5395.3 | 5257.2 | 5188.0 | 5297.5 | 5200.0 | 5202.0 |
| Low coverage grassland (LCGL) | 3220.1 | 2913.9 | 2756.8 | 2688.7 | 2933.1 | 3126 |
| Water area | 177.9 | 146.7 | 90.4 | 76.7 | 63.3 | 150.6 |
| Swamp land | 92.2 | 73.3 | 66.8 | 64.3 | 53.1 | 50.3 |
| Dune sand | 1064.0 | 1608.1 | 1904.2 | 1758.7 | 1547.0 | 1344.1 |
| Saline land | 270.5 | 286.5 | 364.1 | 382.1 | 398.5 | 316.2 |
| Arable land | 4.7 | 14.0 | 20.2 | 15.2 | 24.2 | 24.1 |
| Residential land | 4.0 | 4.5 | 6.3 | 6.2 | 6.2 | 7.1 |
| Transportation land | 26.9 | 29.7 | 36.2 | 40.1 | 42.4 | 45.8 |

Table 5 LCCI change in QLB from 1977 to 2013

| Year | 1977 | 1987 | 2000 | 2007 | 2010 | 2013 |
|-----------------------------------|-------|-------|-------|-------|-------|-------|
| Land cover condition index (LCCI) | 29.74 | 28.83 | 27.70 | 27.78 | 28.57 | 29.18 |
| LCCI rate of change (%) | | −3.06 | −3.92 | 0.29 | 2.84 | 2.14 |

occurred from 1977 to 2000, but there has been a recovery since 2000 (Fig. 3). The specific changes in land cover conversion and spatial distribution differed among land cover types, indicating that the level of degradation and restoration of the eco-environment also differed.

During 1977–1987, the main land cover change was a severely localized desertification around the Sumos of Zhagusty, Uritutala, and Saiinhodog, and upstream of the Gogusty River and the Engeer River sub-catchment (Fig. 4). Table 6 shows that 530.1 km² of LCGL transformed into dune sand, 129.1 and 252 km² of HCGL and MCGL, respectively, deteriorated into MCGL and LCGL, and 83.6 km² of woodland deteriorated into grassland. The area of vegetation degradation was 1055.8 km², accounting for 7.4% of the watershed. Subsequent vegetation recovery has occurred over an area of just 188.3 km². This reflects the net reduction in woodland, grassland degradation, and dune sand expansion and indicated the severe deterioration in the local eco-environment. At the same time, the extent of vegetation degradation and desertification has increased in the OSL (Li et al. 2008; Peng et al. 2007).

From 1987 to 2000, the area of dune sand increased by 296.1 km² (Table 4), equivalent to a watershed-wide expansion rate of 22.8 km²/a. The total area expanded to 1904.2 km² in the southern QLB and the upper reaches of the Gogusty River. There was a large area of mobile dunes in Saiinhodog Sumo and Uritutala Sumo (Fig. 4). The area of saline land increased by 77.6, and 163.1 km² area of HCGL and MCGL declined, and the area of wetland also decreased by 62.8 km². These changes resulted in severe grassland degradation and a decline in pasture quality, seriously damaging the regional eco-environment, and the rate of change in the LCCI was −3.92% (Table 5). Overall, approximately 75% of the area was degraded during this period, causing a rapid deterioration in the OSL eco-environment (Liu et al. 2008). In addition, the area of residential and transportation land increased significantly, due to the intensification of human activity.

In 2000–2007, the eco-environment in the QLB appeared to be recovering. The area of HCGL and MCGL increased by 92.5 and 109.5 km², respectively. Although 485.9 km² of land transitioned to sandy land, 631.4 km² (Table 7) of dune sand was stabilized with preliminary revegetation around the Saiinhodog Sumo (Fig. 4), resulting in the LCCI having an upward trend. At the same time, the local wetland ecosystem was severely degraded. For example, the West Qehan Lake (WQL) dried up completely in 2002, causing the water area to decrease and creating an area of barren saline land in the northern QLB.

During 2007–2010, 381.6 km² of dune sand was transformed into grassland in the western and southern watershed. Although the area of water and swamp land decreased by 13.4 and 11.2 km², respectively, the area that was revegetated (298.9 km²) was larger than the area that was degraded.

The area of dune sand was reduced by 202.9 km², with 189.2 km² of dune sand transformed into LCGL in the western and central watershed areas during 2010–2013. The WQL was restored (Fig. 3). The water area thus grew by 87.3 km², while the area of saline land decreased by 82.3 km². The LCCI rose to 29.18, indicating a considerable improvement in the eco-environment.

Discussion

Analysis of driving forces

The application of PCA using SPSS indicated that land cover change was affected by six factors in the QLB. Three major eigenvalues (PCS1, PCS2, and PCS3) were found to explain 96.32% of the variability. Variables that exhibited a loading > 0.7 were considered to be significant, and their eigenvalues are given in Table 8. PCS1 explained 42.2% of the total variance and was mainly influenced by precipitation and windy days. The factors representing

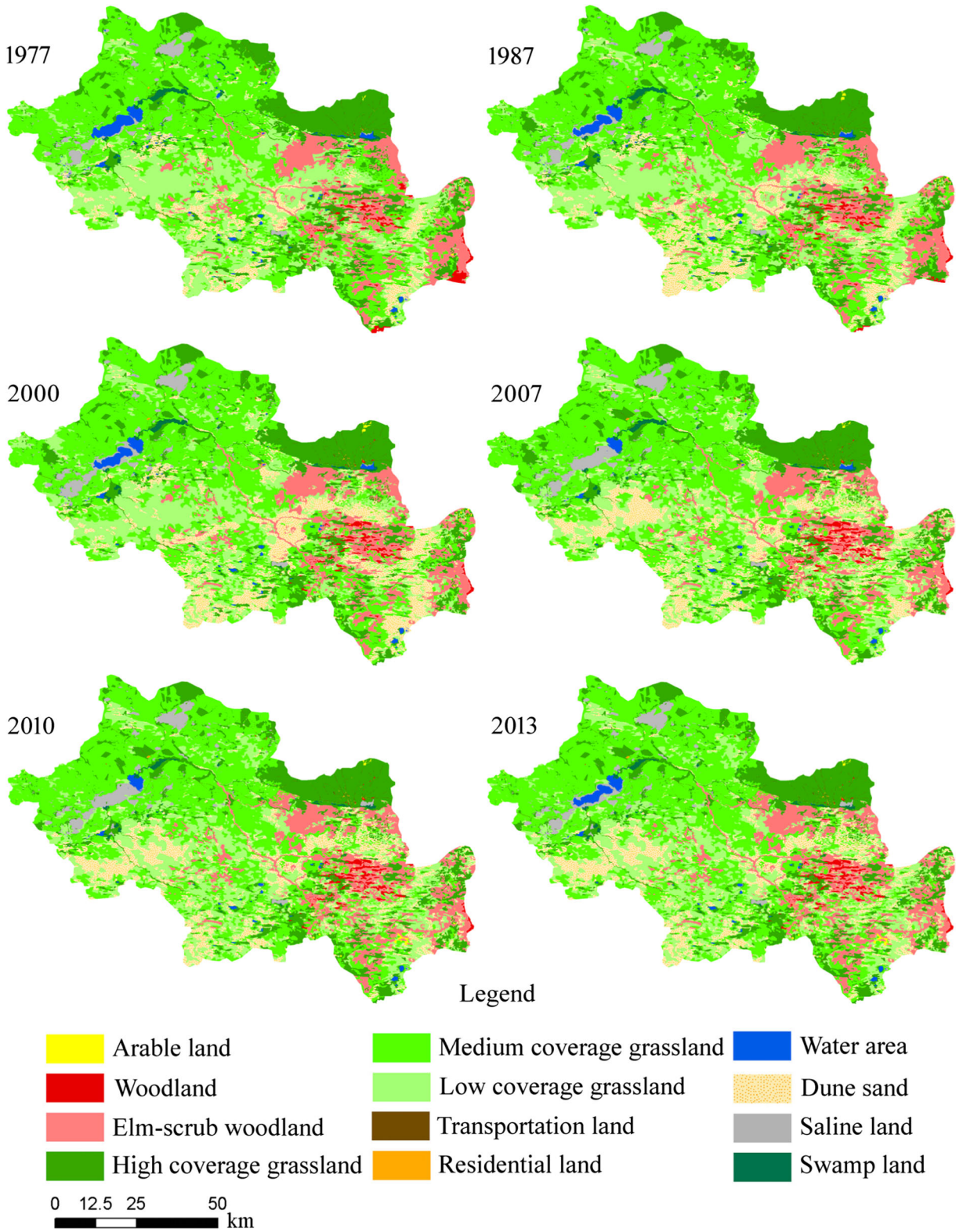


Fig. 3 Land cover change in QLB from 1977 to 2013

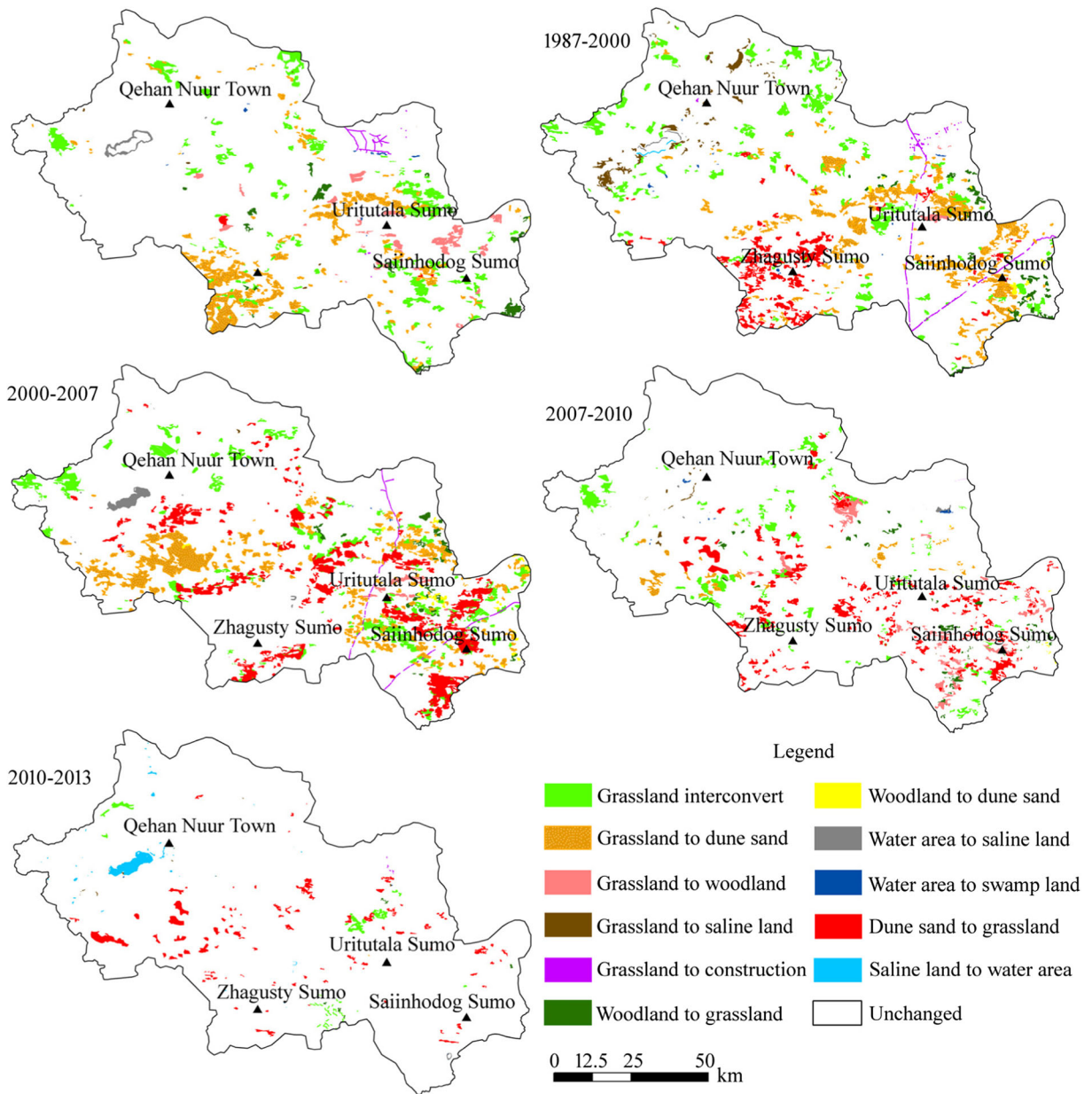


Fig. 4 Temporal and spatial land cover patterns from 1977 to 2013 in the QLB

major climatic change (especially precipitation) played a significant role in eco-environmental changes in the watershed. PCS2 accounted for 34.7% of the total variance and had high loadings for population. PCS3 was defined by livestock numbers, contributing 19.4% of the total variance. Hence, PCS2 and PCS3 suggested that LULC change was substantially influenced by human activity in QLB during 1977–2013.

Correlation between LCCI and PCA factors

Climate change

Land cover change is affected not only by the long-term climatic changes, but also by inter-annual temperature and precipitation variability. In 1955–1976, the mean MAT and MAP in the four meteorological stations used in the study were 1.5 °C and 299.2 mm, respectively,

Table 6 Land cover transfer matrix from 1977 to 1987 in the QLB (unit: km²)

| Land cover type | Wood land | Elm-scrub woodland | HCGL | MCGL | LCGL | Water area | Swamp land | Dune sand | Saline land | Arable land | Residential land | Transportation land | 1977 |
|---------------------|-----------|--------------------|--------|--------|--------|------------|------------|-----------|-------------|-------------|------------------|---------------------|----------|
| Woodland | 89.4 | 0 | 27.6 | 6.0 | 1.3 | 0 | 0 | 0.6 | 0 | 0 | 0 | 0 | 124.9 |
| Elm-scrub woodland | 0 | 1492.7 | 6.7 | 38.4 | 3.6 | 0 | 0 | 0.8 | 0 | 1.0 | 0.2 | 0 | 1543.4 |
| HCGL | 13.3 | 2.8 | 2121.5 | 129.1 | 8.9 | 0 | 0 | 0.3 | 1.0 | 8.2 | 0.2 | 2.7 | 2288.0 |
| MCGL | 3.9 | 24.9 | 51.1 | 5039.9 | 251.9 | 0 | 0 | 22.9 | 0.5 | 0.1 | 0.1 | 0 | 5395.3 |
| LCGL | 0 | 7.4 | 1.2 | 36 | 2645.4 | 0 | 0 | 530.1 | 0 | 0 | 0 | 0 | 3220.1 |
| Water area | 0 | 0 | 5.3 | 0 | 0 | 146.6 | 3.7 | 0.1 | 22.2 | 0 | 0 | 0 | 177.9 |
| Swamp | 0 | 0 | 23.7 | 0 | 0 | 0.1 | 68.3 | 0 | 0 | 0 | 0 | 0.1 | 92.2 |
| Dune sand | 0 | 2.3 | 0.8 | 7.8 | 0 | 0 | 0 | 1053.1 | 0 | 0 | 0 | 0 | 1064 |
| Saline land | 0 | 0 | 3.4 | 0 | 2.8 | 0 | 1.3 | 0.2 | 262.8 | 0 | 0 | 0 | 270.5 |
| Arable land | 0 | 0 | 0 | 0 | 0 | 0 | 0 | 0 | 0 | 4.7 | 0 | 0 | 4.7 |
| Residential land | 0 | 0 | 0 | 0 | 0 | 0 | 0 | 0 | 0 | 0 | 4.0 | 0 | 4.0 |
| Transportation land | 0 | 0 | 0 | 0 | 0 | 0 | 0 | 0 | 0 | 0 | 0 | 26.9 | 26.9 |
| 1987 | 106.6 | 1530.1 | 2241.3 | 5257.2 | 2913.9 | 146.7 | 73.3 | 1608.1 | 286.5 | 14.0 | 4.5 | 29.7 | 14,211.9 |

Table 7 Land cover transfer matrix from 2000 to 2007 in the QLB (unit: km²)

| Land cover type | Woodland | Elm-scrub woodland | HCGL | MCGL | LCGL | Water area | Swamp land | Dune sand | Saline land | Arable land | Residential land | Transportation land | 2000 |
|---------------------|----------|--------------------|--------|--------|--------|------------|------------|-----------|-------------|-------------|------------------|---------------------|----------|
| Woodland | 103.8 | 0 | 1.5 | 0 | 0 | 0 | 0 | 0 | 0 | 0.1 | 0 | 0 | 105.4 |
| Elm-scrub woodland | 0 | 1507.3 | 1.9 | 3.4 | 1.3 | 0 | 0 | 10.5 | 0 | 0.8 | 0 | 0.9 | 1526.1 |
| HCGL | 7.6 | 23.3 | 2099.3 | 15.2 | 2 | 0 | 0 | 0 | 0 | 0 | 0 | 0 | 2147.4 |
| MCGL | 0 | 0 | 94.9 | 4887.5 | 159.1 | 0 | 0 | 36.3 | 8.4 | 0 | 0 | 1.8 | 5188 |
| LCGL | 0 | 0 | 14.9 | 239 | 2060.9 | 0 | 0 | 439.1 | 2 | 0 | 0 | 0.9 | 2756.8 |
| Water area | 0 | 0 | 3.4 | 0 | 0 | 76.7 | 1.1 | 0 | 7.6 | 1.6 | 0 | 0 | 90.4 |
| Swamp land | 0 | 0 | 3.6 | 0 | 0 | 0 | 63.2 | 0 | 0 | 0 | 0 | 0 | 66.8 |
| Dune sand | 0 | 0 | 13.3 | 152.4 | 465.4 | 0 | 0 | 1272.8 | 0 | 0 | 0 | 0.3 | 1904.2 |
| Saline land | 0 | 0 | 0 | 0 | 0 | 0 | 0 | 0 | 364.1 | 0 | 0 | 0 | 364.1 |
| Arable land | 0.5 | 0 | 7.1 | 0 | 0 | 0 | 0 | 0 | 0 | 12.6 | 0 | 0 | 20.2 |
| Residential land | 0 | 0 | 0 | 0 | 0 | 0 | 0 | 0 | 0 | 0.1 | 6.2 | 0 | 6.3 |
| Transportation land | 0 | 0 | 0 | 0 | 0 | 0 | 0 | 0 | 0 | 0 | 0 | 36.2 | 36.2 |
| 2007 | 111.9 | 1530.6 | 2239.9 | 5297.5 | 2688.7 | 76.7 | 64.3 | 1759 | 382.1 | 15.2 | 6.2 | 40.1 | 14,211.9 |

Table 8 Principal component analysis of driving factors component matrix and variance explained in the QLB

| variables | PCS1 | PCS2 | PCS3 |
|-------------------|--------|--------|--------|
| Livestock numbers | 0.423 | 0.463 | -0.774 |
| Population | 0.387 | -0.861 | -0.156 |
| Temperature | 0.564 | -0.689 | 0.356 |
| Precipitation | -0.888 | 0.294 | 0.353 |
| Wind speed | 0.678 | 0.507 | 0.499 |
| Wind days | 0.799 | 0.555 | 0.203 |
| Eigenvalue | 2.532 | 2.082 | 1.165 |
| Proportion (%) | 42.204 | 34.706 | 19.411 |
| Cumulative (%) | 42.204 | 76.910 | 96.320 |

which indicates relatively cold and wet conditions. Studies in the 1960s and 1970s reported that mobile dunes in the OSL accounted for just 2.3 and 8.2% of the total area, respectively (Li et al. 2008), indicating that dune sand was relatively stable and the vegetation cover was still in a good condition.

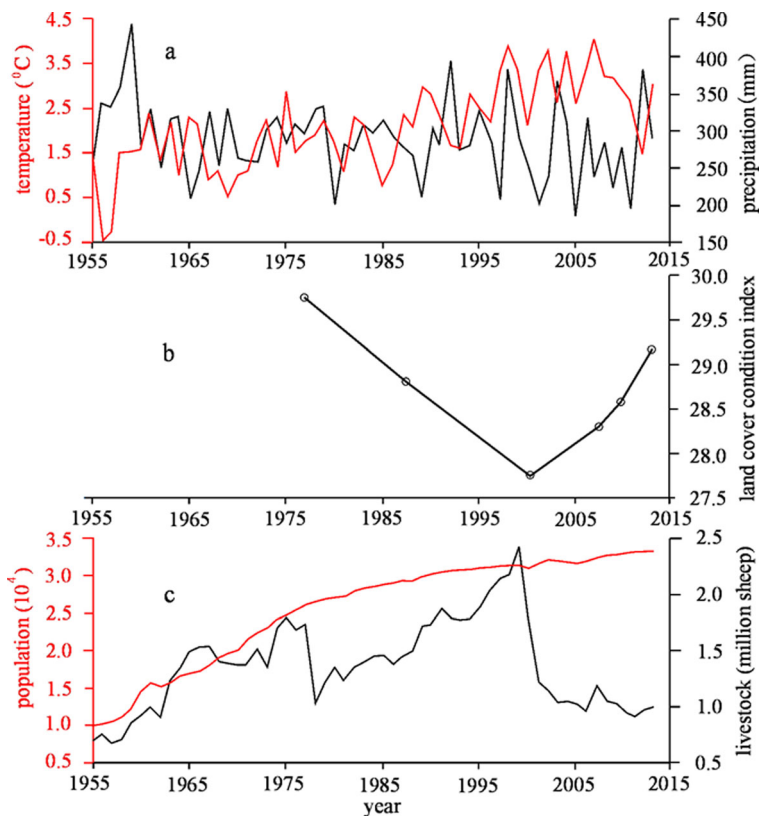
The MAT was 1.8 and 2.2 °C in the watershed in 1977 and 2000, respectively, while the MAP was 299.7

and 248.3 mm, i.e., a decrease of 51.4 mm, indicating a more prominent warming and a lower precipitation trend during 1977–2000 (Fig. 5a). The decreasing LCCI was negatively correlated with a climatic drying trend (Fig. 5a–b). The LCCI declined to a low of 27.7 in 2000 (Fig. 5b), suggesting that the eco-environment had deteriorated seriously (Fig. 6a–c).

Severe, consecutive drought events occurred in 1999, 2000, and 2001. The number of days per annum with wind speed of force 8 or above were 9, 19, and 25, respectively, and there were 2, 4, and 12 sandstorms (Wen 2008), respectively, resulting in a further deterioration of the grassland areas. This enlarged the dune sand area, resulting in a further decline in the LCCI. The PCA results proved that windy days played an important role in land cover change in the watershed. Recent studies have demonstrated that dune sand expansion and grassland degradation reflected the eco-environmental deterioration in this period (Li et al. 2008; Liu et al. 2008; Fang et al. 2004; Bu 2005).

Grassland vegetation has gradually been restored, the wetland area has greatly increased, and the area of dune sand has reduced. This has led to a significant

Fig. 5 The change of MAT (red line) and MAP (dark line) (a), the land cover condition index (b), and livestock numbers (dark line) and population (red line) (c) in QLB



improvement in the LCCI during 2000–2013 (Fig. 6d–f), indicating that eco-environmental function and structure has improved. From the meteorological site records at Abaga and Sunitezuo, the MAP was 384.5 and 272.2 mm in 2012, i.e., 145.4 and 82.1 mm greater than during 1955–2011, respectively. A greater MAP and fewer windy days has led to an increase in the LCCI.

Population

The catchment population displayed a rising trend during 1955–2013 (Fig. 5c). However, there is a significant difference in various periods.

In 1977–2000, there was an increasing trend in the population of the QLB, with the population growth curve negatively correlated with the LCCI. The increasing population has placed pressure on the eco-environment. The population tended to be steady during 2000–2013, which was coupled with an improvement in the LCCI. This suggested that under the implementation of strict ecological protection measures, human activity

has imposed less pressure on the catchment environment.

Pasture loading capacity

The curve in Fig. 5c shows the changes in the number of livestock in the study area and clearly shows three peaks and three low values. The three peaks occurred when the number of livestock reached 1.54, 1.79, and 2.41 million in 1967, 1975, and 1999, respectively. The three low values reflected the severe snowstorms experienced in 1968, 1977, and 2001 when livestock numbers fell sharply to 1.41, 1.05, and 1.16 million, respectively.

Livestock numbers increased rapidly by 1.36 million during 1977–1999 and were negatively correlated with the LCCI (Fig. 5b, c). This suggested that the large number of livestock was placing pressure on the environment and agreed with the PCA results (Table 8). The number of livestock reached a sustainable level of about 1 million during 2000–2013, and the pressure on pasture land was controlled at an appropriate level. Overgrazing

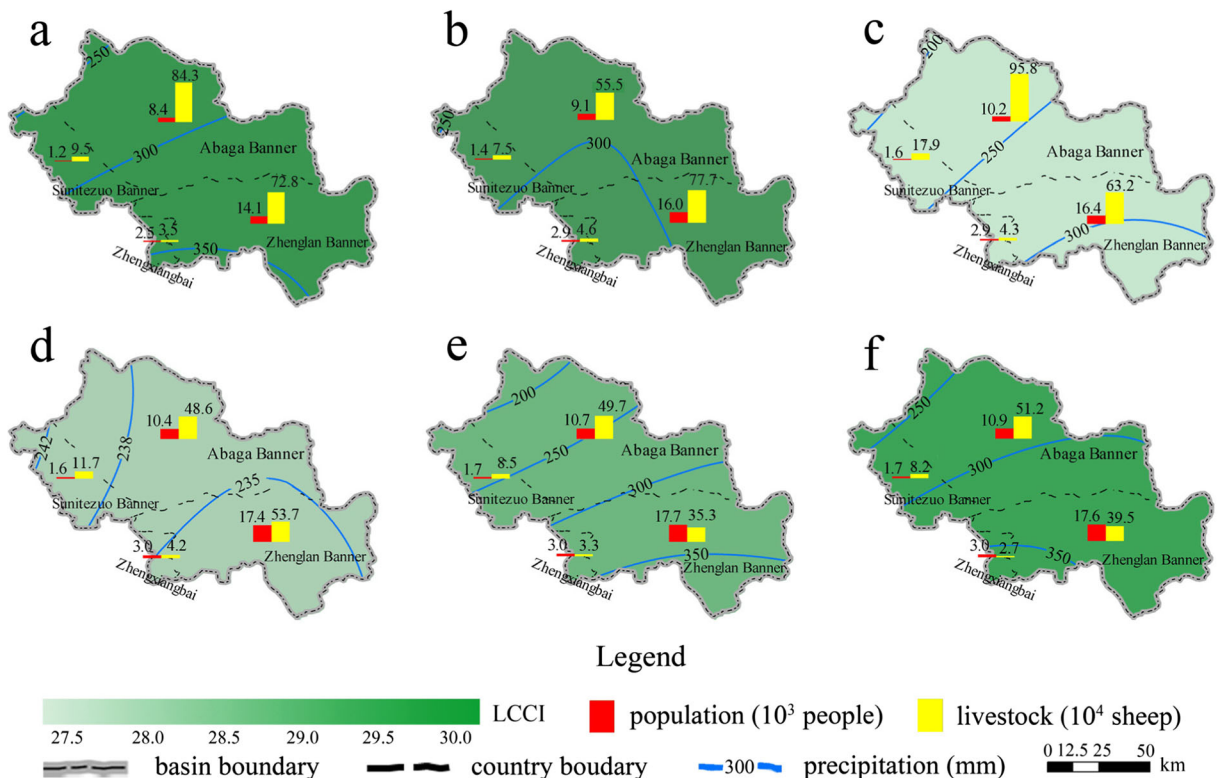


Fig. 6 Spatio-temporal distribution annual precipitation, population, and livestock numbers (a 1977; b 1987; c 2000; d 2007; e 2010; f 2013)

had led to grassland vegetation degradation and a decline in land cover quality (Ma et al. 2005; Wang 2014; Yang et al. 2007), but was not the main reason for eco-environment deterioration. Climate and livestock both have a significant impact on the eco-environment of grassland, but their degree of impact is different. It is clear that the climate played the primary role over a long-time scale. On three occasions, the number of livestock was reduced over a short period due to a natural disaster, suggesting that climate change controlled livestock numbers (Fig. 5c). Therefore, livestock numbers have a capacity for self-adjustment under the process of climate changes.

Policy

Given the economic and ecological benefits, the government needs to draft laws and policies to guide sustainable development during land use transitions. Studies have shown that land management policy has a more significant influence on land use change than any other driving factor (Hua and Squires 2015; Mu et al. 2013; Gao et al. 2016), such as ecological immigration and prohibiting graze (Zhou et al. 2013; Li 2011). The implementation of policies to protect pastures has ensured that grassland resources and livestock maintained a healthy balance during 1955–1966 in Inner Mongolia (Department of Animal Husbandry Compilation History Commission 1997). However, the relaxation of grassland policy led to a large area of grassland being reclaimed for farming during 1967–1978. In 1983, Inner Mongolia implemented the “Livestock and Rangeland Double Contract Responsibility System,” which monitored grazing pasture and livestock subcontracted to each household (Department of Animal Husbandry Compilation History Commission 1997). Driven by economic interests, herdsman fed more livestock to gain income. As livestock numbers and the area of arable land increased rapidly, at the same time rainfall decreased substantially, leading to a decrease in the LCCI. In 2002, the Chinese government began implementing its “Returning Farmland to Forest or Grassland” and “Sandstorm Source Control Project for the Beijing and Tianjin Regions” policies (Wang et al. 2007b; Wu et al. 2013). A grazing prohibition on grassland was implemented in the growing season between April and June every year, which led to a large area of dune sand being stabilized, while the area of HCGL and MCGL increased. The grassland structure and quality improved, which influenced the changes in the LCCI. The

implementation of the “Grain for Green” policy has also played a positive role in ecological protection in the early twenty-first century.

Conclusions

From 1977 to 2013, the area of grassland decreased by 339 km² in the QLB. The area of HCGL, MCGL, and LCGL was reduced by 51.6, 193.3, and 94.1 km², respectively. The area of dune sand and saline land increased by 280.1 and 45.7 km², respectively. The area of woodland increased by 41 km², while the area of wetlands declined by 69.2 km², indicating that the eco-environment remained extremely fragile and unstable. The area of arable land, residential land, and transport land increased considerably, and land use types changed substantially as a consequence of human activity.

There were clear differences in the spatio-temporal pattern of land use and cover. From 1977 to 2000, the area of dune sand extended from the central and southern catchment to the surrounding areas. As a consequence of the implementation of policies and measures designed to ensure ecological protection since 2002, the number of livestock was reduced, grassland vegetation was gradually restored, and the area covered by dune sand was greatly reduced. However, vegetation remains in its preliminary recovery stage in this region.

Over the long term, human activity and climate change factors have influenced the land cover change in the QLB. Precipitation is one of the most important factors in the restoration of the watershed vegetation cover and water area. The role of human activity and land use policies has had an increasing influence on land cover change in recent decades.

Acknowledgements This study was funded by the National Science Foundation of China (No. 41662011 and 41261008) and the National Basic Research Program of China (No. 2012CB426508), and Collaborative innovation center for water environmental security of Inner Mongolia Autonomous region (No. XTCX003).

References

- Bai, Y., Xu, H. L., & Ling, H. B. (2014). Eco-service value evaluation based on eco-economic functional regionalization in a typical basin of northwest arid area, China. *Environmental Earth Sciences*, 71, 3715–3726.

- Brown, C. E. (1998). *Applied multivariate statistics in geohydrology and related sciences*. Berlin: Springer.
- Bu, H. C. L. (2005). Grassland management report. *North Economic, 1*, 5–8 (in Chinese).
- Chen, Z. X., & Zhang, X. S. (2000). Value of ecosystem services in China. *Chinese Science Bulletin, 45*, 870–876.
- Chinese Academy of Sciences Fieldwork group in Inner Mongolia and Ningxia. (1985). *Inner Mongolia of vegetation*. Beijing: Science Press (in Chinese).
- Chun, X., Su, R. G. G., Liu, J. Y., Liang, W. J., Yong, M., & Ulambadrakh, K. (2017). Climatic implications on variations of Qehan Lake in the arid regions of Inner Mongolia during the recent five decades. *Environmental Monitoring and Assessment, 189*, 14. <https://doi.org/10.1007/s10661-016-5721-5>.
- De Coster, J. (1998). *Overview of factor analysis*. Tuscaloosa: Department of Psychology, University of Alabama Retrieved 09/25/2011 from <http://www.stat-help.com/factor.pdf>.
- Department of Animal Husbandry Compilation History Commission. (1997). *Inner Mongolia Autonomous Region. Inner Mongolia livestock events*. Hohhot: Inner Mongolia People's Publish House (in Chinese).
- Fang, J. Y., Piao, S. L., & He, J. S. (2004). Increasing terrestrial vegetation activity in China, 1982–1999. *Science in China (C), 47*, 229–240.
- Gao, L., Kinnucan, H. W., Zhang, Y., & Qiao, G. (2016). The effects of a subsidy for grassland protection on livestock numbers, grazing intensity, and herders' income in Inner Mongolia. *Land Use Policy, 54*, 302–312.
- Hatcher, L. (1994). *A step-by-step approach to using SAS system for factor analysis and structural equation modeling* (pp. 1–56). Cary: SAS.
- Hua, L., & Squires, V. R. (2015). Managing China's pastoral lands: current problems and future prospects. *Land Use Policy, 43*, 129–137.
- Li, J. Y. (2011). The effectiveness of “ecological migration” in reducing poverty (1): a case study based on the Tarim River basin, Xingjiang. *Ecological Migration, (22)*, 137–158. https://doi.org/10.3726/978-3-0351-0206-2_6.
- Li, G. T., Yao, Y. F., & Zuo, H. J. (2008). Study on the relation between growth and site of *Ulmus pumila L.var.sabulosa J.H.Guo* in Otindag sandy land. *World Forest Research, 21*, 82–86 (in Chinese).
- Li, X. Y., Ma, Y. J., & Xu, H. Y. (2009). Impact of land use and land cover change on environmental degradation in Lake Qinghai watershed, northeast Qinghai-Tibet plateau. *Land Degradation & Development, 20*, 69–83.
- Li, J. Y., Xu, B., Yang, X. C., Jin, Y. X., Li, Y. Y., Zhang, J., Zhao, L., & Li, R. L. (2011). Dynamic changes and driving force of grassland sandy desertification in Xilin Gol: a case study of Zhenglan Banner. *Geographical Research, 30*, 1669–1682 (in Chinese).
- Lin, L. J., Dickhoefer, U., Müller, K., Wang, C. J., Glindemann, T., Hao, J., Wan, H. W., Schönbach, P., Gierus, M., Taube, F., & Susenbeth, A. (2012). Growth of sheep as affected by grazing system and grazing intensity in the steppe of Inner Mongolia, China. *Livestock Science, 144*, 140–147.
- Liu, S. L., & Wang, T. (2007). Aeolian desertification from the mid-1970s to 2005 in Otindag Sandy Land, Northern China. *Environmental Geology, 51*, 1057–1064.
- Liu, H. J., Zhou, C. H., Cheng, W. M., Long, E., & Li, R. (2008). Monitoring sandy desertification of Otindag Sandy Land based on multi-date remote sensing images. *Acta Ecologica Sinica, 28*, 627–635.
- Lu, D., Mausel, P., Brondizio, E., & Moran, E. (2004). Change detection techniques. *International Journal of Remote Sensing, 25*, 2365–2401.
- Ma, J. Z., Wang, X. S., & Edmunds, W. M. (2005). The characteristics of groundwater resources and their changes under the impacts of human activity in the arid Northwest China—a case study of the Shiyang River Basin. *Journal of Arid Environments, 61*, 277–295.
- Mason, J. A., Swinehart, J. B., Lu, H. Y., Miao, X. D., Cha, P. A., & Zhou, Y. L. (2008). Limited change in dune mobility in response to a large decrease in wind power in semi-arid northern China since the 1970s. *Geomorphology, 102*, 351–363.
- Matthews, H. D., Weaver, A. J., Meissner, K. J., Gillett, N. P., & Eby, M. (2004). Natural and anthropogenic climate change: incorporating historical land cover change, vegetation dynamics and the global carbon cycle. *Climate Dynamics, 22*, 461–479.
- Mu, S. J., Zhou, S. X., Chen, Y. Z., Li, J. L., Ju, W. M., & Odeh, I. O. A. (2013). Assessing the impact of restoration-induced land conversion and management alternatives on net primary productivity in Inner Mongolian grassland, China. *Global & Planetary Change, 108*, 29–41.
- Niu, S. L., Jiang, G. M., & Wan, S. Q. (2005). Ecophysiological acclimation to different soil moistures in plants from a semi-arid sand land. *Journal of Arid Environments, 63*, 353–365.
- Olofsson, P., Foody, G. M., Herold, M., Stephen, S. V., Woodcock, C. E., & Wulder, M. A. (2014). Good practices for estimating area and assessing accuracy of land change. *Remote Sensing of Environment, 148*, 42–57.
- Peng, Y., Jiang, G. M., & Liu, X. H. (2007). Photosynthesis, transpiration, water use efficiency of four plant species with grazing intensities in Hunshandake Sandland, China. *Journal of Arid Environments, 70*, 304–315.
- Petrisor, A. I., Ianos, I., Iurea, D., & Vaidianu, M. (2012). Applications of principal component analysis integrated with GIS. *Procedia Environmental Sciences, 14*, 247–256.
- Veldkamp, A., & Lambin, E. F. (2001). Predicting land-use change. *Agriculture Ecosystems & Environment, 85*, 1–6.
- Verburg, P. H., Neumann, K., & Nol, L. (2011). Challenges in using land use and land cover data for global change studies. *Global Change Biology, 17*(2), 974–989.
- Wang, T. (2014). Aeolian desertification and its control in Northern China. *International Soil & Water Conservation Research, 2*, 34–41.
- Wang, X. M., Chen, F. H., & Dong, Z. B. (2006). The relative role of climatic and human factors in desertification in semiarid China. *Global Environmental Change, 16*, 48–57.
- Wang, X. H., Lu, C. H., & Fang, J. F. (2007a). Implications for development of grain- for-green policy based on cropland suitability evaluation in desertification-affected north China. *Land Use Policy, 24*, 417–424.
- Wang, X. M., Eerden, H., & Zhou, Z. (2007b). Significance of variations in the wind energy environment over the past 50 years with respect to dune activity and desertification in arid and semiarid northern China. *Geomorphology, 86*, 252–266.

- Wang, X. M., Yang, Y., & Dong, Z. (2009). Responses of dune activity and desertification in China to global warming in the twenty-first century. *Global & Planetary Change*, *67*, 167–185.
- Wen, K. G. (2008). *Chinese meteorological disasters ceremony (Inner Mongolia)*. Beijing: China Meteorological Press (in Chinese).
- Wu, Z. T., Wu, J. J., Liu, J. H., He, B., Lei, T. J., & Wang, Q. F. (2013). Increasing terrestrial vegetation activity of ecological restoration program in the Beijing-Tianjin sand source region of China. *Ecological Engineering*, *52*, 37–50.
- Xiao, X., Ojima, D. S., Parton, W. J., Chen, Z., & Chen, D. (1995). Sensitivity of Inner Mongolia grasslands to climate change. *Journal of Biogeography*, *22*, 643–648.
- Xie, G. D., Zheng, L., & Lu, C. X. (2010). Applying value transfer method for eco-service valuation in China. *Journal of Resources and Ecology*, *1*, 51–59.
- Xu, Z. M., Cheng, G. D., Zhang, Z. Q., Su, Z. Y., & Loomis, J. (2003). Applying contingent valuation in China to measure the total economic value of restoring ecosystem services in Ejina region. *Ecological Economy*, *44*, 345–358.
- Yan, C. Z., Zhou, Y. M., Song, X., & Duan, H. C. (2009). Estimation of areas of sand and dust emission in the Hexi corridor from a land cover database: an approach that combines remote sensing with GIS. *Environmental Geology*, *57*, 707–713.
- Yang, X., Ding, Z., Fan, X., Zhou, Z., & Ma, N. (2007). Processes and mechanisms of desertification in northern China during the last 30 years, with a special reference to the Hunshandake Sandy Land, eastern Inner Mongolia. *Catena*, *71*, 2–12.
- Ye, D. Z., Zhou, J. F., & Liu, J. Y. (2000). Causes of sand-stormy weather in northern China and control measures. *Acta Geographica Sinica*, *55*, 513–552 (in Chinese).
- Yin, H., Pflugmacher, D., Li, A., Li, Z. G., & Hostert, P. (2018). Land use and land cover change in Inner Mongolia—understanding the effects of China’s re-vegetation programs. *Remote Sensing of Environment*, *204*, 918–930.
- Yu, M., Ellis, J. E., & Epstein, H. E. (2004). Regional analysis of climate, primary production, and livestock density in Inner Mongolia. *Journal of Environmental Quality*, *33*, 1675–1681.
- Zhao, H. L., Zhao, X. Y., Zhou, R. L., Zhang, T. H., & Drake, S. (2005). Desertification processes due to heavy grazing in sandy rangeland, Inner Mongolia. *Journal of Arid Environments*, *62*, 309–319.
- Zhao, R. F., Chen, Y. N., & Shi, P. J. (2013). Land use and land cover change and driving mechanism in the arid inland river basin: a case study of Tarim River, Xinjiang, China. *Environmental and Earth Science*, *68*, 591–604.
- Zheng, Y. R., Xie, Z. X., Robert, C., Jiang, L. H., & Shimizu, H. (2006). Did climate drive ecosystem change and induce desertification in Otindag sandy land, China over the past 40 years. *Journal of Arid Environments*, *64*, 523–541.
- Zhou, L., Zhu, Y., Yang, G., & Luo, Y. (2013). Quantitative evaluation of the effect of prohibiting grazing policy on grassland desertification reversal in northern China. *Environmental Earth Sciences*, *68*(8), 2181–2188.